Numerical study on the serviceability performance of reinforced glulam beams with different steel arrangements

Estudo numérico do desempenho em serviço de vigas MLC armadas com diferentes arranjos do aço

Lucas Sacramoni Peixoto
Julio Soriano
William Martins Vicente
Nilson Tadeu Mascia

Abstract

Glued laminated timber (glulam) beams manufactured with glued steel bars can achieve improvements in their mechanical performance and the effects of the arrangement of steel bars in the cross-section are of technological interest. This study aimed to evaluate the mechanical behavior of beams with symmetric reinforcements (compression and tension zones) and beams with asymmetric reinforcements (compression zone), under loading imposed at the serviceability limit state. To achieve this goal, glulam beams with reinforcement ratios ranging from 0.5% to 4% were simulated using the finite element method. When compared to the nonreinforced beams it was found for the deflections that the asymmetric reinforcements provided reductions of up to 31.5% and the cases with symmetric reinforcements were more efficient, with deflection reductions of up to 45%. In comparison to the symmetric arrangement of the bars, the asymmetric distribution provided a reduction of up to 10.5% in the normal stress of the glulam beam compression zone. The asymmetrically arranged reinforcement effectively contributed to increasing the stiffness of the beam and was more efficient in reducing normal stresses in the compressive zone, thus preventing the initial yielding of the wood.

Keywords: Glued laminated timber. Steel bars. Bending. Finite element method.

Resumo

As vigas de madeira lamelada colada (MLC) fabricadas com barras de aço coladas podem alcançar melhorias no seu desempenho mecânico e os efeitos da disposição das barras de aço na seção transversal são de interesse tecnológico. Esta pesquisa objetivou a avaliação do comportamento mecânico de vigas com reforços simétricos (zonas de compressão e de tração) e vigas com reforços assimétricos (zona de compressão), sob condições de carregamento impostas ao estado limite de serviço. Portanto, vigas de MLC com taxas de reforço variando de 0,5% a 4% foram simuladas pelo método dos elementos finitos. Em relação às vigas sem reforços, as flechas das vigas reforçadas assimetricamente resultaram até 31,5% menores e, as vigas com reforços simétricos foram mais eficientes, cuja redução das flechas foi de até 45%. Comparativamente ao arranjo simétrico das barras, a distribuição assimétrica proporcionou uma redução de até 10,5% na tensão normal da zona de compressão da MLC. A armadura disposta de forma assimétrica contribuiu efetivamente para o aumento da rigidez da viga e foi mais eficiente na redução das tensões normais na zona compressiva, evitando com isso o escoamento inicial da madeira.

Palavras-chave: *Madeira lamelada colada. Barras de aço. Flexão. Método dos elementos finitos.*

[1]**Lucas Sacramoni Peixoto**
[1]Universidade Estadual de Campinas
Campinas – SP – Brasil

[2]**Julio Soriano**
[2]Universidade Estadual de Campinas
Campinas – SP – Brasil

[3]**William Martins Vicente**
[3]Universidade Estadual de Campinas
Campinas – SP – Brasil

[4]**Nilson Tadeu Mascia**
[4]Universidade Estadual de Campinas
Campinas – SP - Brasil

Recebido em 30/11/23
Aceito em 24/02/24

Introduction

Advances in technologies for the manufacture of wood products have provided advantages when compared with conventional sawn wood pieces. Among the different products constituted using high-performance adhesives, glued laminated timber (glulam) has several benefits for structural use, such as the manufacture of pieces with large dimensions and different shapes, highlighting curved pieces with variable cross-sections (Mackerle, 2005; Fiorelli; Dias, 2006; Shmulsky; Jones, 2011; Stokke, 2014; Kawecki; Podgórski, 2018; FPL, 2021). In the glulam manufacturing stages, the laminate selection and classification process enables the reduction of the presence of natural and wood drying defects, which consequently results in products with lower variability and better mechanical performance than solid-sawn wood (Moses; Prion, 2004; SFIF, 2016).The Phenol-resorcinol adhesive is mentioned as the most common in the assembly of glulam pieces (Shmulsky; Jones, 2011; FPL, 2021), with melamine-formaldehyde, phenol-formaldehyde and polyurethane adhesives also being used. Faced with concerns about the emissions of substances harmful to human health, such as oil-derived, the search for polyurethane adhesives based on vegetable oil originate from castor beans, and soybeans, among other plants, has been driven (Shirmohammadli *et al.*, 2023).

Additionally, glulam beams can be reinforced to obtain improved properties, such as increased stiffness and mechanical strength, mainly to reduce deflection and increase load capacity (Soriano; Pellis; Mascia, 2016; Ghazijahani; Jiao; Holloway, 2017; Halicka; Ślósarz, 2021). It should be highlighted the possibilities of reinforcement with polymer fibers (Raftery; Harte, 2011; Buligon *et al.*, 2013; D'Ambrisi; Feo; Focacci, 2013; Ghazijahani; Jiao; Holloway, 2017; Mascia *et al.*, 2018), natural fibers (Mascia; Mayer; Moraes, 2014), and steel elements (De Luca; Marano, 2012; Negrão, 2012; Soriano; Pellis; Mascia, 2016).

In the stage preceding the gluing of laminates, steel bars used in reinforced concrete can be rigidly glued to grooves made in laminates of both tensioned and compressed zones. To bond steel elements to wooden pieces, compatible adhesives must be used, such as epoxy and polyurethane (FPL, 2021). The bars substantially improve the beam stiffness, with the benefits of reducing deflections and increasing loading capacity (De Luca; Marano, 2012; Soriano; Pellis; Mascia, 2016; Ghazijahani; Jiao; Holloway, 2017). In turn, the structural performance of these pieces depends on several parameters, such as the mechanical properties of the materials, amount, and arrangement of reinforcement in the cross-section (De Luca; Marano, 2012; Schober *et al.*, 2015).

Wood has a lower compressive strength than tensile strength (Bodig; Jayne, 1993; Green, 2001), which in the case of a bent piece initially causes the yielding of compressed fibers, with consequently increased stress on the tensioned fibers, leading to brittle failure of these fibers. Modifying the brittle failure mode of a wooden piece is, therefore, a benefit achieved with the reinforcement strategy with some type of ductile material applied to the tension zone of the beam. Considering this behavior, studies addressing the effects and efficiency of reinforcements according to their positioning in the cross-section of glulam are of fundamental importance. Experimental tests provide conditions for understanding certain structural behaviors based on the evaluation of prototypes under pre-established methodological conditions, with the breadth and effectiveness of the results strongly dependent on the details of the prototype, the equipment, and the instrumentation used.

One of the technological methods to evaluate the structural performance of reinforced beams is computational modeling using the finite element method (Miotto; Dias, 2012; Zhang *et al.*, 2015; Uzel *et al.*, 2018). Computational modeling has been highlighted as advantageous in overcoming some inherent limitations of experimental tests (Gaff *et al.*, 2015; Gomez-Ceballos; Gamboa-Marrufo; Grondin, 2022; Vilela *et al.*, 2023), providing, for example, faster analysis, less expensive, with ease in repeating and modifying the loading conditions and properties of the structural model. In the analysis of the load-carrying capacity in timber beams strengthened with carbon fiber reinforced polymer (CFRP), Kim and Harries (2010) considered the results obtained by experimental modeling and experimental results to be very representative, with an error of less than 10%. From solid modeling based on a line-elastic model to analysis of unreinforced glulam beams, as well as beams reinforced with prestressed steel bars or synthetic bars, Wdowiak-Postulak (2023) showed good correlations to the experimental results of the reinforced pieces. To glulam beams reinforced with prestressed steel bars under a load level of 10 kN, the author recorded percentage differences for vertical displacements of 1.21%, normal stress for steel equal to 3.98%, and normal stresses in glulam equal to 6.73 and 5.41%, in compression and tension, respectively. Wdowiak-Postulak (2023) attributed that such differences may result from the limitations of the models in representing the total complexity of the wood material. For an analysis that considered the failure behavior of glulam beams reinforced with steel bars, constituted in three distinct groups due to the symmetrical distribution of the bars in the cross-section of the beam, the computational model was adjusted considering the non-linear behavior (XU *et al.*, 2012). As a result, the ultimate moments predicted by the computational analysis to the experimental results presented errors of the order of 2 to 5%, showing a good adjustment of the proposed model.

This study aimed to evaluate the mechanical behavior of glulam beams reinforced with steel bars by the effect of the symmetrical or asymmetrical arrangement in the beam cross-section. To elucidate the importance of the proposed arrangements for steel bars in the performance of this type of engineered wood, under loading imposed at the serviceability limit state, this numerical study was performed. Therefore, the finite element method (FEM) was used to investigate the effects concerning stiffness and normal bending stress.

Materials and methods

Glulam beams with and without reinforcement were simulated, with a cross-section measuring 52 mm (width) and 154 mm (height) and a span equal to 2820 mm, whose dimensions were inspired by experimental research carried out by Pellis (2015), in which glulam beams were manufactured. The reinforced beams formed two groups according to the number of bars. The Group I beams (Figures 1a and 1b) were designed with two steel bars (commercial diameters, ∅ equal to 5, 6.3, 8, 10, and 12.5 mm), and the Group II beams (Figures 1c and 1d) were simulated with four bars (∅ equal to 5, 6.3, 8, and 10 mm). Each beam's cross-section consisted of seven 22 mm thick *Pinus elliottii* laminates. In the reinforced pieces, the bars were positioned with their centroid (y_s) 27 mm distant from the top or bottom of the beam. For the most critical lodging situation, with four bars of 10 mm diameter in a single layer (Figure 1d) and for the width of the beam analyzed, the timber cover for the two sidebars resulted in a maximum of 10.1 mm. According to the experimental study carried out by Pigozzo *et al.* (2023), the anchoring of bars glued to wooden pieces has full connection efficiency with the minimum distance from the face of the piece to the center of the bar equal to 1.5∅. Additionally, the bars arranged on the same glue line must have a minimum center-to-center distance equal to 2∅. When this distance limit is not respected, Pigozzo *et al.* (2023) report that for groups of three or four bars, the anchoring resistance is reduced to 90%, compared to anchoring with one or two bars. In this case, alternatively, the arrangement of two grouped bars or multiple layers can be adopted.

Following the static scheme proposed in D198-14 (ASTM, 2014) and adopted by Pellis (2015), the beams were simulated with the concentrated load (P/2) applied at the third point of the span (Figure 2).

Figure 1 - **Cross-sections and geometric parameters of the beams simulated with two bars (Group I) and four bars (Group II) - (a) Symmetric reinforcement with two bars; (b) Asymmetric reinforcement with two bars; (c) Symmetric reinforcement with four bars; and (d) asymmetric reinforcement with four bars**

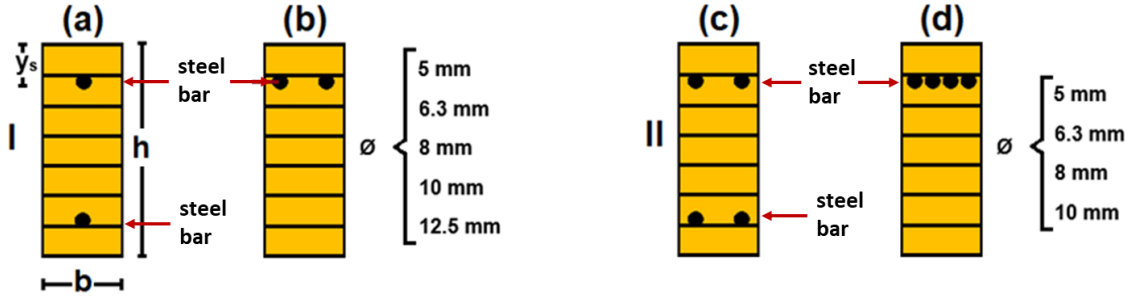

Figure 2 - **Static scheme of the simulated and tested beams**

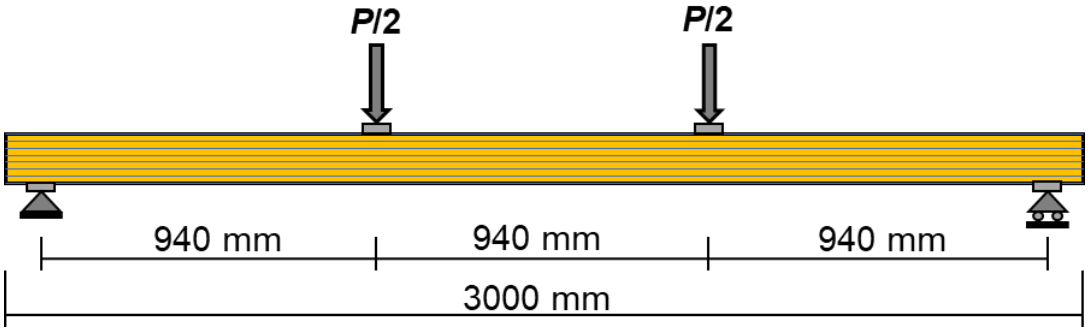

The reinforcement ratios were defined based on the range from 0.2 to 4%, which are values used in the experimental study (De Vecchi *et al.*, 2008; Pellis, 2015) and based on the commercial diameters of steel bars. Thus, the beams were simulated with ratios of reinforcement of 0.25 to 3% (Group I) and 0.5 to 4% (Group II).

Materials specification

The orthotropic properties of wood are truly relevant in detailed studies, such as in analyses of the behavior of joints or the effects of the presence of knots. The general bending behavior, in terms of stiffness and normal stress in glulam beams, is strongly determined by the parallelism of the grain to the larger axis of the piece. In this case, some simplifications can be assumed for the theoretical models, such as the transverse isotropy (Xu; Bouchair; Racher, 2012; Fossetti; Minafo; Papia, 2015) or isotropic models (Fiorelli; Dias, 2011; Gaspar; Cruz; Gomes, 2011; Yang *et al.*, 2016; Neilson *et al.*, 2021). For this purpose, in the dynamic analysis of timber bridges using FEM, for the model of glulam beams, Neilson *et al.* (2021) employed the isotropic model, with a modulus of elasticity equal to 13,000 MPa. In the theoretical model studied by Yang *et al.* (2016), for the flexural behavior of gulam beams reinforced with steel or fiber-reinforced polymer (FRP), for the glulam material, a general value of the modulus of elasticity equal to 10,760 MPa was used.

In this study, the wood was admitted with a modulus of elasticity parallel to the grain (E_L) equal to 12,435 MPa and density equal to 537 kg m^{-3}, values that were obtained experimentally at a moisture content of 10.5% (Pellis, 2015). Poisson's ratios: $\nu_{(Longitudinal\text{-}Radial)}$ and $\nu_{(Longitudinal\text{-}Tangential)}$ were adopted equal to 0.4 (Table 1), representing a mean of the values shown for several pine species (FPL, 2021). Based on the mechanical properties parallel to the fibers of the species *Pinus elliottii* (Calil Junior *et al.*, 2006, Reis; Faria, 2009; Torquato, 2019), the mean compressive strength ($f_{c0,med}$) and the mean tensile strength ($f_{t0,med}$) were adopted (Table 1). For the usual steel bars for reinforced concrete, with a density equal to 7850 kg m^{-3}, the mechanical properties were used according to NBR 7480 (ABNT, 2022a).

According to NBR 7190-1 (ABNT, 2022b), structural adhesives must have properties compatible with the environmental conditions of use of the piece, in the related service class, to ensure the integrity of the connection during the expected life of the piece. Bonding parameters must meet the manufacturer's specifications with the recommendation of using certified adhesives (ABNT, 2022c). Based on the development of experiments and the literature cited, the use of polyurethane-based adhesives is suggested for gluing wooden lamellas (Soriano; Pellis; Mascia, 2016; Pellis; Soriano; Ferrari, 2017; Kržišnik *et al.*, 2020). For gluing steel bars and wood, it is suggested to use epoxy or polyurethane-based adhesive (Pellis; Soriano; Ferrari, 2017; Pigozzo *et al.*, 2023).

Determination of loading range and bending stiffness

In the simulation of bent timber pieces, for the tensioned zone, the linear elastic model is commonly used to represent the stress–strain relationship ($\sigma \times \varepsilon$), and for the compressed zone, the model usually has three phases: elastic, elastoplastic, and plastic. In a study with redwood pine (*Pinus sylvestris L.*), the initial yield stress was represented within the range from 60 to 70% of the ultimate compressive stress parallel to the grain (Baño *et al.*, 2011). For Radiata pine (*Pinus radiata*), the relationship between the proportionality stress and the maximum stress in compression parallel to the grain was 76.2% (Franke; Quenneville, 2013).

Table 1 - **Materials and their corresponding mechanical properties**

Material	Compressive strength (MPa)[i]	Tensile strength (MPa)[i]	Modulus of elasticity (MPa)	Poisson's ratio (dimensionless)
Glulam	40.4	66.0	12,435.0	0.4
Steel	500.0 (600.0)[ii]	500.0 (600.0)[ii]	210,000.0	0.3

Source: adapted from Calil Junior *et al.* (2006), Reis and Faria (2009), Pellis (2015), Torquato (2019), FPL (2021) and NBR 7480 (ABNT, 2022a).
Note: [i]Mean compressive($f_{c0,med}$) and tensile strength ($f_{t0,med}$) parallel to the grain of glulam; characteristic yield strength of steel (f_{yk}).[ii]Bars with a diameter of 5 mm available in steel with f_{yk} = 600.0 MPa and for the other diameters steel with f_{yk} = 500.0 MPa.

The modulus of elasticity in bending is given within a linear range of the load–deflection curve, and therefore, in this study, the corresponding range of 10-50% of the maximum load was assumed. For the compressive strength parallel to the grain equal to 40.4 MPa and the tensile strength parallel to the grain equal to 66 MPa, in the interval from 10-50%, the values for compression result equal 4.04 MPa ($\sigma_{10\%}$) and 20.2 MPa ($\sigma_{50\%}$) and, for tension 6.6 MPa ($\sigma_{10\%}$) and 33 MPa ($\sigma_{50\%}$). With the values common to both intervals and to guarantee the linear elastic behavior, both in the tensioned zone and in the compressed zone, the interval of 6.6 MPa and 20.2 MPa was adopted for the modeling.

Based on these considerations, to determine the maximum normal stress on the timber and the deflections, the beams without reinforcement and reinforced with four bars of 10 mm diameter (Figure 1c) were simulated with an incremental load. With this procedure, a loading range was established, for which the stresses were concerned in the linear elastic phase. Concomitantly, to comply with the Serviceability Limit State (SLS), the deflection was limited to $L/200$ (equal to 14.1 mm). According to NBR 7190-1 (ABNT, 2022b) and BS EN 1995-1-1 (BSI, 2014), for a beam on two supports, the limit value for the final deflection (composed of the instantaneous and creep deformations) must be within the range of $L/150$ to $L/300$. To determine the beams' stiffness increments, with a static scheme according to D198-14 (ASTM, 2014), Equation 1 was used.

$$E_L \cdot I = \frac{\mathbf{23} \cdot \boldsymbol{\Delta P} \cdot \boldsymbol{L^3}}{\mathbf{1296} \cdot \boldsymbol{\Delta u}} \quad \text{Eq. 1}$$

Where:

ΔP is the load increment (kN);

L is the span (m);

Δu is the deflection increment (m);

I is the second moment of inertia (m^4); and

E_L is the modulus of elasticity (kN m^{-2}).

Modeling by the finite element method

Using Ansys software (2020), a total of ten beams (Group I) and eight beams (Group II) were simulated, with three-dimensional models prepared in the Workbench module. The manually generated meshes (Figure 3) were discretized with three-dimensional elements Solid186, formed by 20 nodes and with three degrees of freedom per node (displacement according to the *X*, *Y*, and *Z* axes). As a design principle, Porteous and Kermani (2007) describe having no slippage between elements that form the glued composite sections. The contact surface between steel and glulam considered perfect adhesion (without slippage) was modeled with the Targe170 and Conta174 elements.

For a better approximation of the static conditions of the tested beams, the supports were supposed to be under blocks (Figures 3b and 3c) modeled with Solid186 elements, which adhered to the beams and simulated a metal plate for better distribution of stresses on the support zones (Xu; Bouchair; Racher, 2012; Uzel *et al.*, 2018). This device was also used in the zones of concentrated load ($P/2$), which are theoretically punctual in the third point of the beam span.

The least refined mesh was generated in the beam without reinforcement, counting a total of 2321 nodes and 990 elements, and the most refined mesh was generated in the beam with symmetric reinforcement of four bars of 10 mm in diameter, which totaled 104,000 nodes and 59,530 elements. This increase in the number of nodes and elements for the second case was due to the insertion of the steel bars and their contact with the wood material. For each case of simulated structure, the acceptance of their respective meshes occurred through evaluation of the approximations of the resulting normal stresses at the top and bottom of the beams, as well as in the steel bars in their respective positions (compressed and tensioned zones). For each applied mesh, these maximum normal stresses were taken in the cross-section at the midspan of the beams, with decimal precision being acceptable as convergent.

To evaluate the differences between symmetric and asymmetric reinforcement, the maximum normal stress at the edges of the tensioned and compressed zones was determined, as well as the stress on the steel bars of all configurations.

Figure 3 - **Mesh generated with three-dimensional elements type Solid186: (a) Glulam beam, (b) Support zone of the asymmetrically reinforced glulam beam and (c) Support zone of the symmetrically reinforced glulam beam**

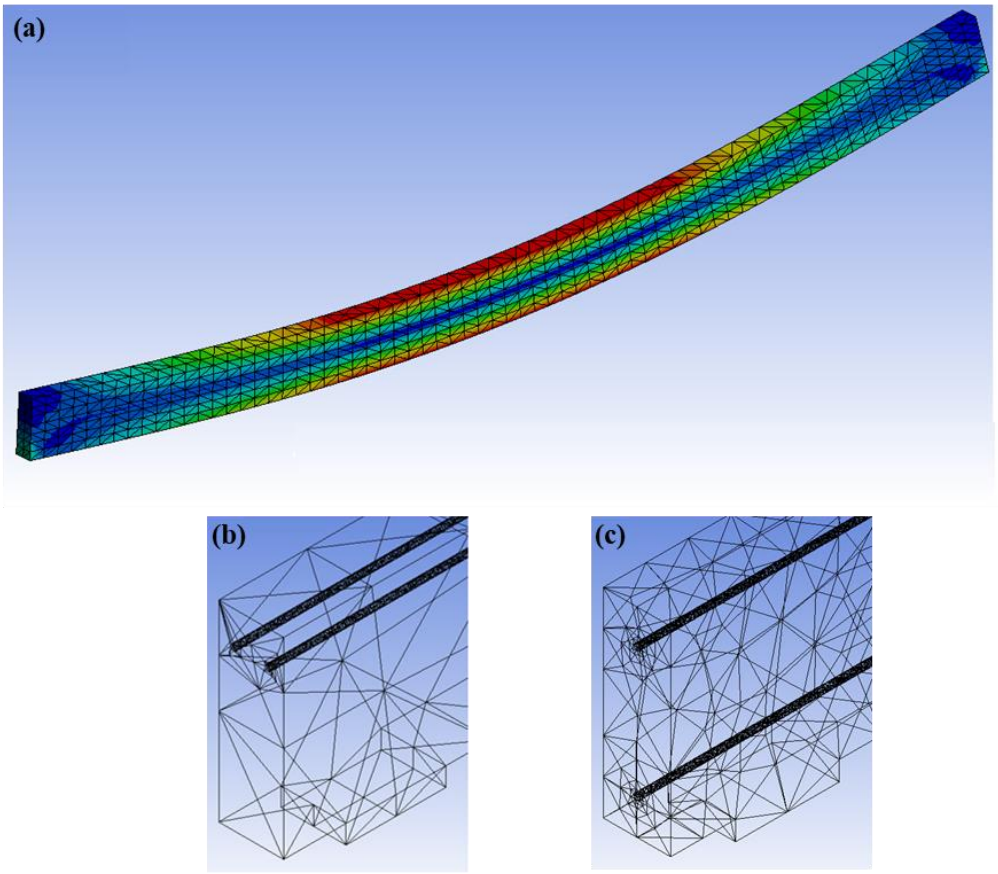

Results and discussion

Loading range

The methodology and scope of this study focused on the behavior of the beams in the linear elastic phase, with normal stresses (σ) ranging from 6.6 to 20.2 MPa, and simulating the pieces up to the condition of maximum reinforcement ratio (four bars of 10 mm diameter), the values of 5 and 9 kN were established for the loading range (Figure 4).

Concerning the SLS, it was determined that the loading for the limit deflection is a function of beam span (L/200 = 14.1 mm). For the beam with lower stiffness (glulam), a load value of approximately 7 kN was obtained (Figure 5). This value resulted in less than 9 kN, showing, for the conditions of this research, that the limit deflection occurred in the elastic phase. In the design procedures, to comply with the ultimate limit state (ULS), the design strength of the wood (f_{wd}) must take into account the characteristic strength ($f_{wk} = 0.7 \times f_{w,med}$), the partial factor ($\gamma_w$) and the modification factor (k_{mod}). The value of γ_w depends on the nature of the effort and the modification factor is composed of two factors k_{mod1} and k_{mod2}, whose values and details can be seen in NBR 7190-1 (ABNT, 2022b). The k_{mod1} is defined for five load-duration classes, ranging from 0.6 to 1.1. Concerning the compressive stress, with γ_w equal to 1.4, depending on the different combinations of design conditions, the design strength results from 8.48 to 22.22 MPa.

To comply with both conditions exposed as the methodology of this research, the loading range adopted for modeling both groups of beams was established from 5 to 7 kN, so that all pieces presented maximum stress in linear elastic behavior and, simultaneously, that the deflection for the established limits (BSI, 2014; ABNT, 2022b) was not exceeded.

Figure 4 - **Load-normal stress curves for glulam elements of nonreinforced and reinforced beams**

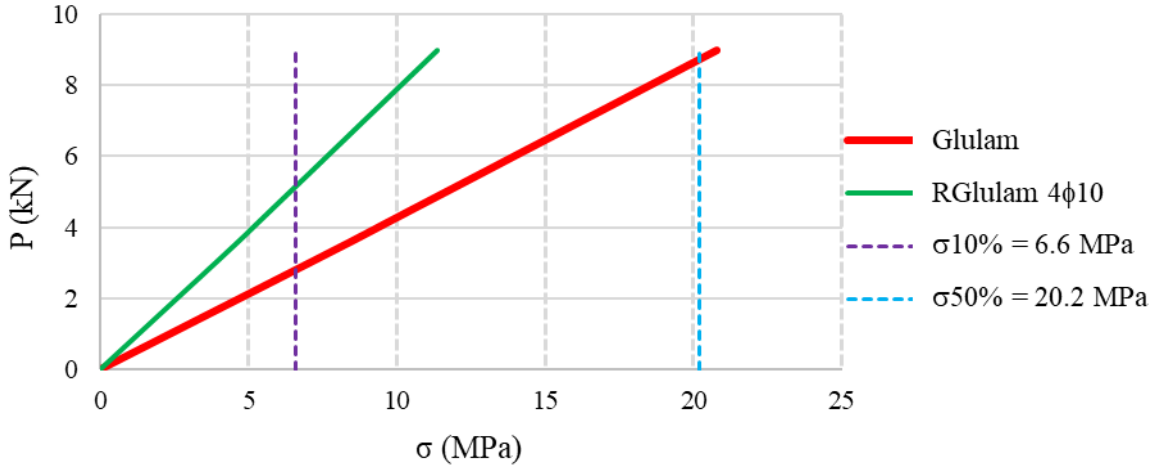

Figure 5 - **Load–deflection curves for nonreinforced and reinforced beams**

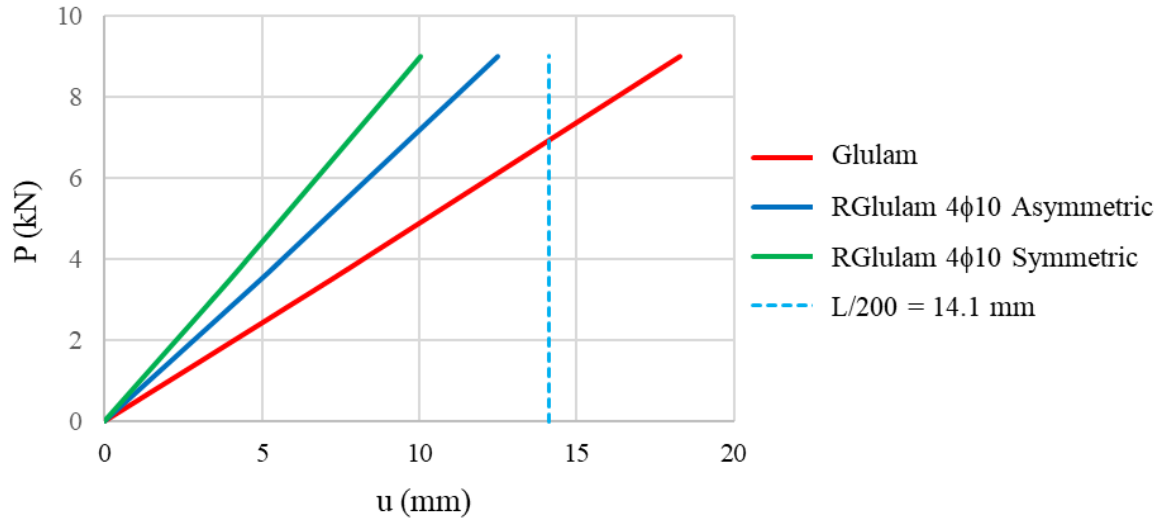

Effects resulting from symmetric and asymmetric reinforcements

The beam with a reinforcement ratio equal to 4%, compared with the case of the nonreinforced beam, provided deflection reductions on the order of 45% and 31.5% for the bars arranged symmetrically and asymmetrically, respectively. With these results, the symmetric arrangement was more advantageous, providing higher stiffness to the reinforced glulam beam (Figure 5).

As a result of the reinforcement, an increase of 38% in the stiffness of glulam beams was experimentally obtained by De Luca and Marano (2012), who used for this purpose a prestressed steel bar in the tensioned zone and another in the compressed zone, amounting to a reinforcement ratio equal to 0.82%. With this reinforcement system, the authors also recorded a 40% increase in the load capacity of the beams. The efficiency of the reinforcement system in glulam beams with internally glued prestressed steel bars, regarding increased stiffness and load capacity, was also confirmed by Negrão (2012).

The stress values obtained by computational modeling (Figure 6) illustrate how the reduction in maximum normal stress in reinforced glulam beams is influenced by the reinforcement ratio (ρ) and by the arrangement of the bars in the cross-section. For glulam beams symmetrically reinforced with ρ equal to 4%, about the nonreinforced glulam beams, the maximum normal stress, both at the top and bottom of the beam, was reduced from 11.6 to 6.4 MPa, i.e., these significant reductions were equal to 45% (Figures 6a and 6c). For the asymmetric configuration, the reduction in normal compressive stress resulted in an equal 48%.

The results for asymmetric bar arrangement (Figure 6b), compared with the case of symmetric bar arrangement (Figure 6a), showed the effects of reduced normal stress on glulam elements of the compressed zone, as well as reduced normal stress on the steel bars (Figures 6e and 6f). On the other hand, still comparing the results for the asymmetric and symmetric arrangements, in all cases, there was increased maximum normal stress in glulam elements of the tensioned edge (Figures 6c and 6d). These results show that the asymmetric arrangement of reinforcement is a solution to be considered when compression stress reduction is needed to prevent failure by yielding on the compressed fibers of the timber.

Figure 6 - **Normal stress-reinforcement ratio curves at the edges of the beams and steel bars for a loading equal to 5 kN: (a) Glulam at the top of the beam with symmetric reinforcement, (b) Glulam at the top of the beam with asymmetric reinforcement, (c) Glulam at the bottom of the beam with symmetric reinforcement, (d) Glulam at the bottom of the beam with asymmetric reinforcement, (e) Steel bars in a symmetric arrangement and (f) Steel bars in an asymmetric arrangement**

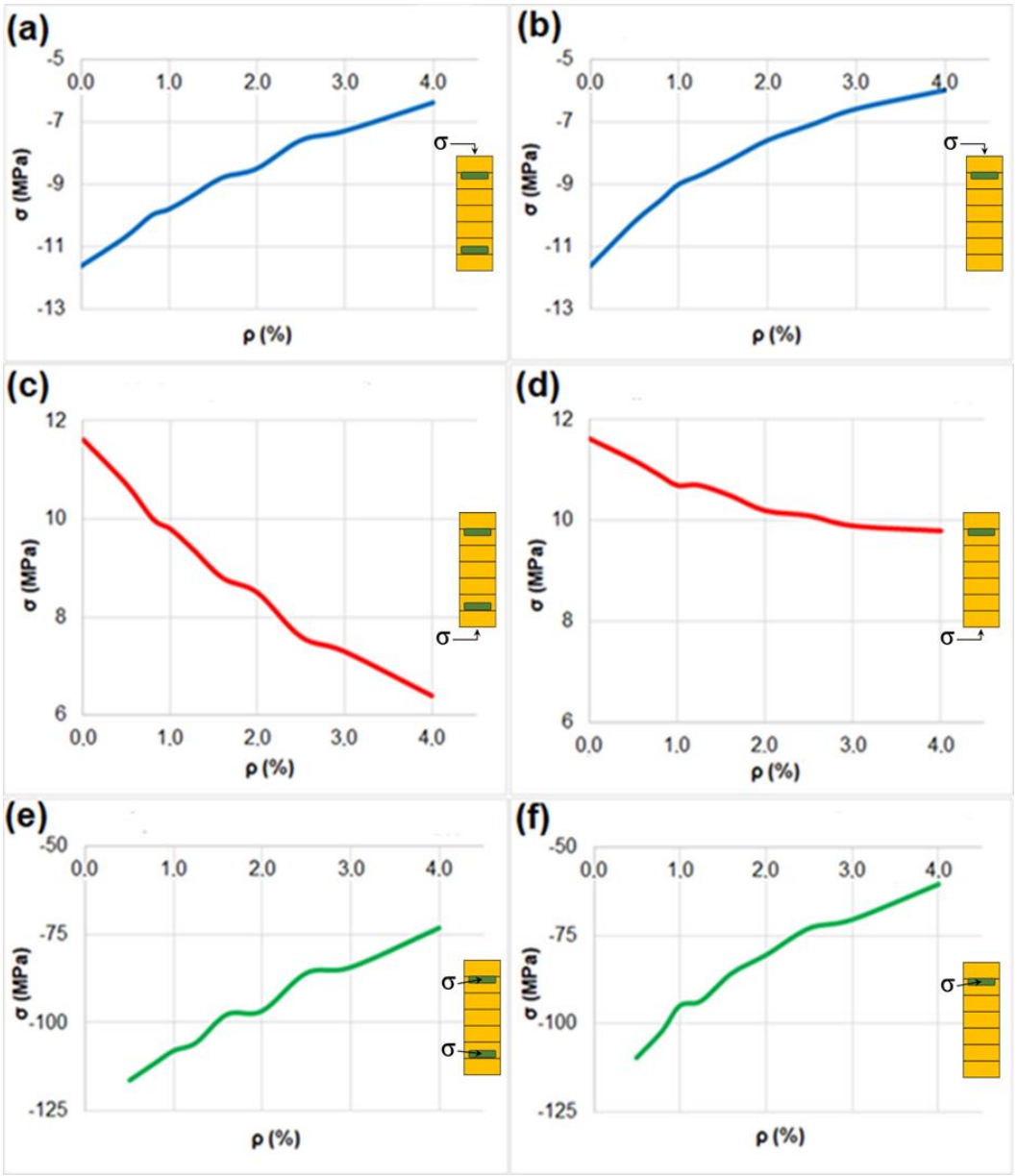

The normal stress at the top of the beam with asymmetric reinforcement, about the symmetric arrangement (Figures 6b and 6a), considering all reinforcement ratios, was reduced to a mean value of 0.5 MPa. In the steel bars, also positioned at the top of the beam, the mean reduction in normal stress obtained with the asymmetric arrangement was equal to 12 MPa (Figures 6f and 6e). Because the value of the modulus of elasticity of steel (E_s) is higher than that of wood (E_L), the reductions in normal stress in the steel bars were more significant for the asymmetric arrangement and the higher reinforcement ratios.

The behavior of a wood beam described by Bodig and Jayne (1993) and Green (2001) shows that the brittle failure of the tensioned fibers occurs at a stage after reaching the limit of the compressive strength parallel to the grain, which characterizes the yielding followed by failures of these compressed fibers. Thus, by reducing the compression stress parallel to the grain and, consequently, the possibility of increments for the loading of the beam, the asymmetric reinforcement configured a better arrangement for the steel bars.

Stiffness increase

The stiffness gain of a reinforced beam is strongly influenced by the modulus of elasticity of the reinforcing material. In general, the materials chosen for reinforcement have a modulus of elasticity much higher than that of wood, which in this case and based on the values in Table 1 resulted in a modular ratio E_s/E_L equal to 16.9.

The results for stiffness obtained as a function of the increase in the reinforcement ratio (Equation 1), represented by a quadratic function (Figure 7), for reinforcement ratios of up to 1% show that the increase in stiffness was practically linear, and from this value of reinforcement ratio, the stiffness increase rate tends to decay notably up to 4%. Equaling to zero the first derivative of the quadratic function that represents this behavior, the maximum stiffness of 285.4 kN m^2 is obtained for a reinforcement ratio equal to 4.6%, whose stiffness gain with the nonreinforced beam ($E_L \cdot I$ = 197.2 kN m^2) is 44.7%. This extrapolation of the adjustment function shows that the highest reinforcement ratio (4%) used in the modeled beams was remarkably close to that of the maximum efficiency of the reinforcement.

The effect of stiffness represented in Figure 7 due to the reinforcement ratio imposed as asymmetric reinforcement can also be seen in terms of the reduction in deflection for both arrangement groups (I and II). For the loading of 7 kN, the glulam reinforced with 2% steel led to a reduction of 3.3 mm in deflection (Figure 8). However, as the reinforcement increased from 2% to 4%, the deflection decreased by only 1.1 mm, showing that the increase in stiffness varied nonlinearly with the increase in reinforcement ratio.

The evaluation of stiffness as a parameter of the mechanical performance of a bent beam clearly showed by the results of this study the benefits of reinforcing glulam beams. In addition to the stiffness provided, which can also be obtained by other types of reinforcements, such as synthetic or natural fibers (Mascia; Mayer; Moraes, 2014), steel bars can also be used for reinforcing the compression region of the wood. Thus, the reinforcement technique with asymmetrically arranged steel bars adds greater possibilities for the optimization of glulam beams, considering both the needed stiffness and the susceptibility to yielding on the compression side of the beam.

Figure 7 - **Stiffness-reinforcement ratio curve for the asymmetrically reinforced beams**

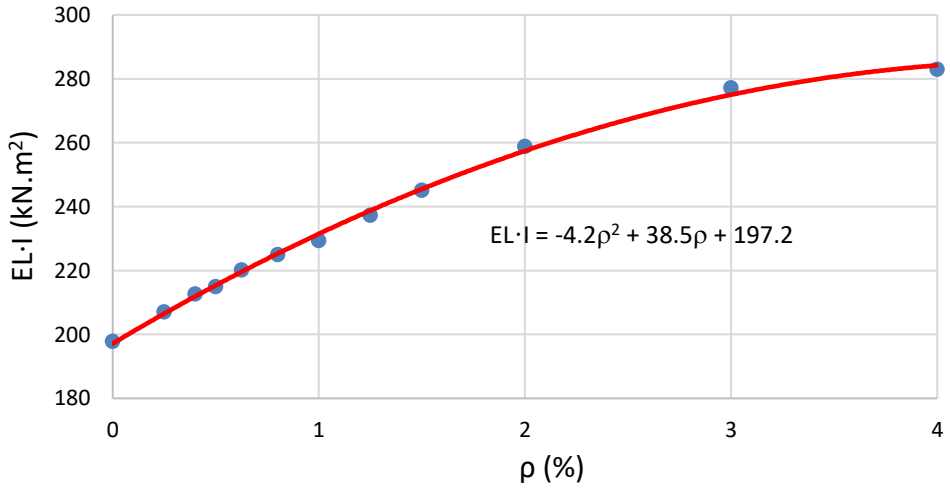

Figure 8 - **Load–deflection curves for nonreinforced beams and asymmetrically reinforced beams with reinforcement ratios equal to 2% and 4%**

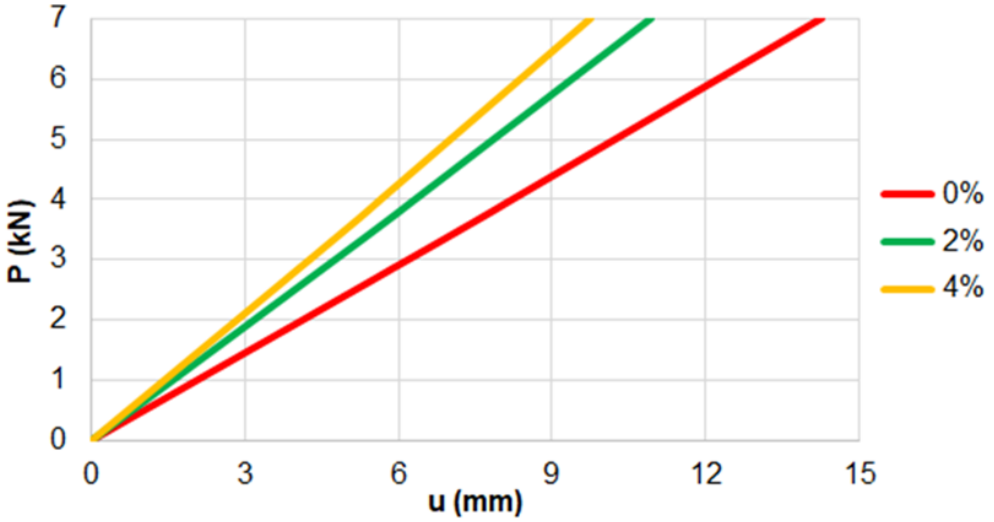

Final remarks

Considering the development of this research in the scope of linear elastic behavior for the imposed conditions of SLS and the numerical model used with isotropic properties, more complex models must be implemented in continuation of this research, such as transverse isotropy, as well as the behavior nonlinearity of materials for stress levels above proportionality limits. However, corroborating with Wdowiak-Postulak (2023), in addition to the usual simplifications in engineering practices, small differences in the numerical modeling results are expected since is impossible to consider all the complexities of the wood material.

In a previously carried out research, which aimed to evaluate the homogenization of the cross-section of symmetrically reinforced glulam beams with computational modeling procedures similar to those used here, Peixoto *et al.* (2022) obtained a good agreement between the numerical and experimental results in the analysis of vertical displacements and maximum normal stresses. However, the research must be expanded with other stages of experimental tests so that in all cases studied, a detailed comparative analysis of the results obtained by numerical models with the experimental results can be carried out.

Conclusions

The effects resulting from the positioning of steel bars inserted in the cross-section of glulam beams, simulated by the finite element method, were significant for the increase in the mechanical performance of the reinforced pieces. For the beams evaluated with the highest ratio of reinforcement (equal to 4%) and with the bars arranged asymmetrically and symmetrically, the deflection was reduced by 31.5% and 45%, respectively.

The asymmetric configuration of the reinforcement, compared with the symmetric reinforcement, reduced by up to 10.5% the normal stress in the glulam elements of the compressed zone, being, therefore, a more efficient arrangement to prevent the failure that initializes by yielding the wood fibers in this zone.

The stiffness increases and normal stress reduction in the compressed zone wood elements varied nonlinearly with the increase in reinforcement ratio. For both studied parameters, the variations obtained in their results were less significant when the reinforcement ratio was closer to 4%, the maximum value employed.

References

AMERICAN SOCIETY FOR TESTING AND MATERIALS. **D198-14**: standard test methods of static tests of lumber in structural sizes. West Conshohocken, 2014.

ANSYS. **ANSYS Release 19.2**. ANSYS Academic Research Mechanical, 2020.

ASSOCIAÇÃO BRASILEIRA DE NORMAS TÉCNICAS. **NBR 7190-1**: projeto de estruturas de madeira: parte 1: critérios de dimensionamento. Rio de Janeiro, 2022b.

ASSOCIAÇÃO BRASILEIRA DE NORMAS TÉCNICAS. **NBR 7190-6**: projeto de estruturas de madeira: parte 6: métodos de ensaio para caracterização de madeira colada estrutural. Rio de Janeiro, 2022c.

ASSOCIAÇÃO BRASILEIRA DE NORMAS TÉCNICAS. **NBR 7480**: aço destinado às armaduras para estruturas de concreto armado: requisitos. Rio de Janeiro, 2022a.

BAÑO, V. *et al.* Prediction of bending load capacity of timber using a finite element method simulation of knots and grain deviation. **Biosystems Engineering**, v. 109, p. 241-249, 2011.

BODIG, J.; JAYNE, B. A. **Mechanics of wood and wood composites**. Melbourne: Frieger Publishing Company Malabar, 1993.

BRITISH STANDARDS INSTITUTION. **BS EN 1995-1-1:2004+A2:** Eurocode 5: design of timber structures: part 1-1: general: common rules and rules for buildings. London, 2014.

BULIGON, E. A. *et al.* Physical and mechanical properties of laminated veneer lumber reinforced GFRP. **Ciência Florestal**, v. 25, n. 3, p. 731-741, 2013.

CALIL JUNIOR, C. *et al*. **Manual de projeto e construção de pontes de madeira**. São Carlos: Suprema, 2006.

D'AMBRISI, A.; FEO, L.; FOCACCI, F. Experimental and analytical investigation on bond between Carbon-FRCM materials and masonry. **Composites Part B: Engineering**, v. 46, p. 15-20, 2013.

DE LUCA, V.; MARANO, C. Prestressed glulam timbers reinforced with steel bars. Construction and Building Materials, v. 30, n. 1, p. 206-217, 2012.

DE VECCHI, A. *et al.* Reinforced Glulam: An innovative building technology. **International Journal for Housing Science**, v. 32, n. 3, p. 207-211, 2008.

FIORELLI, J.; DIAS, A. A. Fiberglass-reinforced glulam beams: mechanical properties and theoretical Model. **Materials Research**, v. 9, n. 3, p. 263-269, 2006.

FIORELLI, J.; DIAS, A. A. Glulam beams reinforced with FRP externally-bonded: theoretical and experimental evaluation. **Materials and Structures**, v. 44, n. 8, p. 1431–1440, 2011.

FOREST PRODUCTS LABORATORY. **Wood handbook**: wood as an engineering material. Madison: Department of Agriculture, Forest Service, Forest Products Laboratory, 2021. General Technical Report FPL-GTR-190.

FOSSETTI, M.; MINAFO, G.; PAPIA, M. Flexural behaviour of glulam timber beams reinforced with FRP cords. **Construction and Building Materials**, v. 95, p. 54–64, 2015.

FRANKE, S.; QUENNEVILLE, P. Compression behavior and material parameters of radiata pine at different orientations to the grain. **Journal of Materials in Civil Engineering**, v. 25, n. 10, p. 1514-1523, 2013.

GAFF, M. *et al.* Stress simulation in layered wood-based materials under mechanical loading. **Materials & Design**, v. 87, p. 1065-1071, 2015.

GASPAR, F.; CRUZ, H.; GOMES, A. Predicting delamination influence on the mechanical performance of straight glued laminated timber beams. In: INTERNATIONAL CONFERENCE ON STRUCTURAL HEALTH ASSESSMENT OF TIMBER STRUCTURES, 11., Lisbon, 2011. **Proceedings [...]** Lisbon: LNEC, 2011.

GHAZIJAHANI, T. G.; JIAO, H.; HOLLOWAY, D. Composite timber beams strengthened by steel and CFRP. **Journal of Composites for Construction**, v. 21, n. 1, 04016059, 2017.

GOMEZ-CEBALLOS, W. G.; GAMBOA-MARRUFO, M.; GRONDIN, F. Multi-criteria assessment of a high-performance glulam through numerical simulation. **Engineering Structures**, v. 256, 114021, 2022.

GREEN, D. W. Wood: strength and stiffness. In: BUSCHOW, J. K. H. *et al.* (ed.). **Encyclopedia of materials**: science and technology. Amsterdam: Elsevier, 2001.

HALICKA, A.; ŚLÓSARZ, S. Strengthening of timber beams with pretensioned CFRP strips. **Structures**, v. 34, p. 2912-2921, 2021.

KAWECKI, B.; PODGÓRSKI, J. Numerical and experimental research on delamination of glulam elements. **Archives of Civil Engineering**, v. 64, n. 3, p. 15-29, 2018.

KIM, Y. J.; HARRIES, K. A. Modeling of timber beams strengthened with various CFRPcomposites. **Engineering Structures**, v. 32, p. 3225–3234, 2010.

KRŽIŠNIK, D. *et al*. Durability and mechanical performance of differently treated glulam beams during two years of outdoor exposure. **Drvnaindustrija**, v. 71, n. 3, p. 243-252, 2020.

MACKERLE, J. Finite element analyses in wood research: a bibliography. **Wood Science and Technology,** v. 39, p. 579–600, 2005.

MASCIA, N. T. *et al.* Numerical analysis of glued laminated timber beams reinforced by Vectran fibers. **Ambiente Construído**, Porto Alegre, v. 18, n. 3, p. 359-373, jul./set. 2018.

MASCIA, N. T.; MAYER, R. M.; MORAES, R. W. Analysis of wood laminated beams reinforced with sisal fibres. **Key Engineering Materials**, v. 600, p. 97-104, 2014.

MIOTTO, J. L.; DIAS, A. A. Evaluation of perforated steel plates as connection in glulam–concrete composite structures. **Construction and Building Materials**, v. 28, n. 1, p. 216-223, 2012.

MOSES, D. M.; PRION, H. G. L. Stress and failure analysis of wood composites: a new model. **Composites: Part B**, v. 35, p. 251–261, 2004.

NEGRÃO, J. H. Prestressing systems for timber beams. In: WORLD CONFERENCE ON TIMBER ENGINEERING, 12., Auckland, 2012. **Proceedings [...]** Auckland: WCTE, 2012.

NEILSON, J. H. *et al.* Experimental and numerical dynamic properties of two timber footbridges including seasonal effects. **International Journal of Civil Engineering**, v. 19, p. 1239–1250, 2021.

PEIXOTO, L. S. *et al.* Bending behavior of steel bars reinforced glulam beams considering the homogenized cross section. **Wood Material Science & Engineering**, v. 17, n. 6, p. 533-539, 2022.

PELLIS, B. P. **Desempenho mecânico de vigas de madeira laminada colada armada confeccionadas com adesivo poliuretânico**. Campinas, 2015. 118 f. Dissertação (Mestrado em Engenharia Agrícola) - Faculdade de Engenharia Agrícola, Universidade Estadual de Campinas, Campinas, 2015.

PELLIS, B. P.; SORIANO, J.; FERRARI, A. M. S. Madeira laminada colada reforçada com barras de aço coladas com epoxi e com poliuretano. In: CONGRESO LATINOAMERICANO DE ESTRUCTURAS DE MADERA; CONGRESO IBERO-LATINOAMERICANO DE LA MADERA EM LA CONSTRUCCION, 2., Junin, 2017. **Prodeedings [...]** Junin: UNNOBA, 2017.

PIGOZZO, J. C. *et al*. Análise de barras de aço ancoradas na madeira utilizando adesivos estruturais. **Ambiente Construído**, Porto Alegre, v. 23, n. 1, p. 145-156, 2023.

PORTEOUS, J.; KERMANI, A. **Structural timber design to Eurocode 5**. Oxford: Blackwell Publishing, 2007.

RAFTERY, G. M.; HARTE, A. M. Low-grade glued laminated timber reinforced with FRP plate. **Composites Part B: Engineering**, v. 42, n. 4, p. 724-735, 2011.

REIS, M. A. P.; FARIA, O. B. Bambu project: mechanical characteristics of the glued laminated bamboo. In: WORLD BAMBOO CONGRESS, 8., Bangkok, 2009. **Proceedings [...]** Bangkok: World Bamboo, 2009.

SCHOBER, K. U. *et al.* FRP reinforcement of timber structures. **Construction and Building Materials**, v. 97, p. 106-118, 2015.

SHIRMOHAMMADLI, Y. *et al.* One-component polyurethane adhesives in timber engineering applications: a review. **International Journal of Adhesion and Adhesives**, v. 123, 103358, 2023.

SHMULSKY, R.; JONES, P. D. **Forest products and wood science**: an introduction. Chichester: Wiley-Blackwell, 2011.

SORIANO, J.; PELLIS, B. P.; MASCIA, N. T. Mechanical performance of glued-laminated timber beams symmetrically reinforced with steel bars. **Composite Structures**, v. 150, p. 200-207, 2016.

STOKKE, D. D. **Introduction to wood and natural fiber composites**. Chichester: Wiley, 2014.

SWEDISH FOREST INDUSTRIES FEDERATION. **Design of timber structures**: structural aspects of timber construction. Stockholm: SFIF, 2016.

TORQUATO, P. H. B. **Estudo do comportamento mecânico de estruturas de madeira laminada colada**. Campinas, 2019. 96 f. Dissertação (Mestrado em Engenharia Mecânica) - Faculdade de Engenharia Mecânica, Universidade Estadual de Campinas, Campinas, 2019.

UZEL, M. *et al.* Experimental investigation of flexural behavior of glulam beams reinforced with different bonding surface materials. **Construction and Building Materials**, v. 158, p. 149-163, 2018.

VILELA R. *et al.* Mechanical performance analysis in bending of glulam beams reinforced with synthetic Vectranfibres. **Ambiente Construído**, Porto Alegre, v. 23, n. 4, p. 289-302, out./dez. 2023.

WDOWIAK-POSTULAK, A. Numerical, theoretical and experimental models of the static performance of timber beams reinforced with steel, basalt and glass pre-stressed bars. **Composite Structures**, v. 305, 116479, 2023.

XU, B. H.; BOUCHAIR, A.; RACHER, P. Analytical study and finite element modelling of timber connections with glued-in rods in bending. **Construction and Building Materials**, v. 34, p. 337-345, 2012.

YANG, H. *et al.* Flexural behavior of FRP and steel reinforced glulam beams: experimental and theoretical evaluation. **Construction and Building Materials**, v. 106, p. 550–563, 2016.

ZHANG, J. *et al.* Research on residual bending capacities of used wood members based on the correlation between non-destructive testing results and the mechanical properties of wood. **Journal of Zhejiang University - Science A**, v. 16, n. 7, p. 541-550, 2015.

Lucas Sacramoni Peixoto
Conceptualization, Data curation, Investigation, Methodology, Software, Validation, Writing – original draft.

Faculdade de Engenharia Agrícola | Universidade Estadual de Campinas | Av. Cândido Rondon, 501 | Campinas – SP – Brasil | CEP 13083-875 | Tel.: (19) 3521-1040 | E-mail: lucassacramoni@gmail.com

Julio Soriano
Conceptualization, Formal analysis, Funding acquisition, Investigation, Methodology, Project

Administration, Validation, Supervision, Writing – original draft, Writing – review & editing.

Faculdade de Engenharia Agrícola | Universidade Estadual de Campinas | E-mail: julio.soriano@feagri.unicamp.br

William Martins Vicente
Conceptualization, Formal analysis, Investigation, Methodology, Supervision, Writing – original draft.

Faculdade de Engenharia Agrícola | Universidade Estadual de Campinas | E-mail: william.vicente@feagri.unicamp.br

Nilson Tadeu Mascia
Formal analysis, Supervision, Writing – review & editing.

Faculdade de Engenharia Civil, Arquitetura e Urbanismo | Universidade Estadual de Campinas | Rua Saturnino de Brito, 224 | Campinas – SP – Brasil | CEP 13083-889 | Tel.: (19) 3521-2318 | E-mail: nilson@fec.unicamp.br

Editores: **Marcelo Henrique Farias de Medeiros** e **Julio Cesar Molina**

Ambiente Construído
Revista da Associação Nacional de Tecnologia do Ambiente Construído
Av. Osvaldo Aranha, 99 - 3º andar, Centro
Porto Alegre – RS - Brasil
CEP 90035-190
Telefone: +55 (51) 3308-4084
www.seer.ufrgs.br/ambienteconstruido
www.scielo.br/ac
E-mail: ambienteconstruido@ufrgs.br